Iraqi Journal of Physics, 2023 *Vol. 21, No.2, PP. 9-16*
https://doi.org/10.30723/ijp.v21i2.1092
P-ISSN: 2070-4003
E-ISSN: 2664-5548

Cytotoxic Activity of CuO NPs Prepared by PLAL Against Liver Cancer (Hep-G2) Cell Line and HdFn Cell Lines

Huda H. Abbas[1a*] and Sabah N. Mazhir[1b]
[1]College of Science for Women, University of Baghdad, Baghdad, Iraq
[b]E-mail: sabahnm_phys@csw.uobaghdad.edu.iq
[a*]Corresponding author: hoda.hussein1204a@csw.uobaghdad.edu.iq

Abstract

A simple physical technique was used in this study to create stable and cost-effective copper oxide (CuO) nanoparticles from pure copper metal using the pulsed laser ablation technique. The synthesis of crystalline CuO nanoparticles was confirmed by various analytical techniques such as particle concentration measurement using atomic absorption spectrometry (AAS), field emission scanning electron microscopy (FE-SEM), the energy dispersive X-ray (EDX), and X-ray diffraction (XRD) to determine the crystal size and identify of the crystal structure of the prepared particles. The main characteristic diffraction peaks of the three samples were consistent. The corresponding 2θ is also consistent, and the cytotoxicity of the nanoparticles was also investigated. After 24 hours of exposure, the percentage of cytotoxicity was calculated. The maximum toxicity of Hep-G2 was 37.81% at the maximum concentration of (500) µg mL^{-1} after 24 hours of exposure. Also, the maximum toxicity of the normal cell line was 27.85% at a maximum concentration of (500) µg mL^{-1}.

Article Info.

Keywords:
CuO NPs, PLAL, liver Cancer, HdFn cell lines, Photoluminescence

Article history:
Received: Jan. 01, 2023
Accepted: Apr. 04, 2023
Published: Jun. 01,2023

1. Introduction

There has been an increase demand for nanoparticles, which has resulted from large-scale manufacturers employing high-energy processes and solvents. Nanoparticles exhibit unique electrical, optical, chemical, and biological capabilities [1]. Nanoparticles differ from bulk particles in terms of electrical resistance, chemical reactivity, electrical conductivity, strength and hardness, diffusivity, and biological activity, photovoltaics, heterogeneous catalysis, gas-sensor technologies, nonlinear optics, medicine, and microelectronics [2-6]. For synthesizing nanoparticles, a simple top-down method Pulsed Laser Ablation in liquid (PLAL) was utilized. Among the many advantages of this method is the capacity to manage the size and quality of the generated nanoparticles and the guarantee that they are contaminated-free [7-9]. A range of ablation variables, including laser fluence, pulse width, repetition rate, wavelength, temperature, ablation duration, and the concentration of the stabilizing agent, influence nanoparticles shape, size, and morphology [10]. Researchers are particularly interested in metallic oxide nanoparticles since they are used in various industrial operations and medical and pharmaceutical applications. They can also be used in the manufacture of cosmetics, microelectronic devices, and semiconductors [11-16]. Metal oxide nanoparticles, such as (CuO), have generated interest due to their antibacterial and biocidal properties, and their potential use in a wide range of biomedical applications [17, 18].

Cancer of the liver is the world's third leading cause of cancer death. Liver cancer is a major public health concern because it has such a dramatic impact on our lives.

Fundamental research into the molecular mechanisms of liver cancer is required for long-term and dependable prevention and treatment methods. The cell lines are treated as in vitro equivalents of tumor tissues, making them indispensable for basic cancer research. Certified cell lines retain most of the original tumor's genetic properties and mimic its microenvironment. Hep-G2 is a well-known hepatic cell line. It is used in various scientific research applications, from oncogenesis to the cytotoxicity of substances on the liver [19].

The aim of the study is to prepare copper oxide particles in an economical and inexpensive way and to employ these particles in measuring the cytotoxicity of normal and cancerous cells.

2. Experimental Methods

2.1. CuO Nanoparticles Synthesis

CuO nanoparticles were created in deionized water using a pulsed Q-switched Nd:YAG nanosecond laser with the following parameters: energy = 400 mJ, frequency f = 4, 6, and 8 Hz, wavelength λ = 1064 nm, and the number of pulses = 100 shots. The operation was achieved by placing a (1x1) cm copper plate of (1) mm thickness at the bottom of a quartz container filled with (3) ml of deionized water, as illustrated in Fig.1.

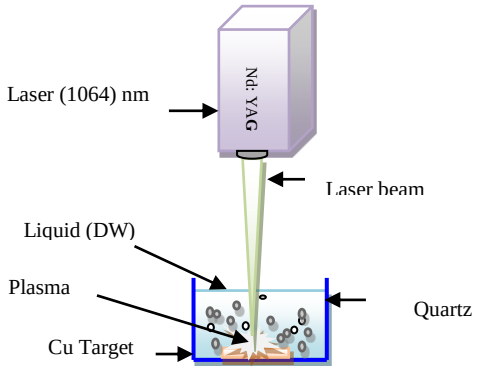

Figure 1: Prepared CuO nanoparticles by PALA.

2.2. Nanoparticles Sample Preparation

The drop method was used to prepare thin films; the solution containing the copper nanoparticles was deposited on a glass slide at room temperature; this was done several times and left to completely dry, thus forming a thin layer on the surface of the glass slide.

Atomic Absorption Spectroscopy (AAS) measures the amount of UV/Visible light energy absorbed by an element. The wavelength of light absorbed corresponds to the energy needed to excite electrons from the ground state to a higher energy level. The amount of energy absorbed in this excitation process is proportional to the concentration of the element in the sample, as shown in Table 1. The Field Effect Scanning Electron Microscope (FESEM), Energy-Dispersion X-ray Spectroscopy (EDX), and X-Ray Diffraction (XRD) were employed to study the characteristics of the prepared thin films.

Table 1. Concentration of CuO NPs by Atomic Absorption.

Sample	Frequency (Hz)	Concentration (µg/ml)
CuO	4	0.7
CuO	6	1.2
CuO	8	1.4

2.3. MTT Assay

10,000 cells from different cell lines were cultured into 96-well plates with different concentrations of CuO NPs and incubated for 24 hours at 37° C in an incubator with 5% CO_2. Also, cells without adding CuO NPS were cultivated to serve as the positive control group. The well without the cells serves as the negative control. After 24 hours, using a sampler, 10 µl of MTT solution was added to 100 µl of cell culture supernatant with gentle shaking by hand or on a shaker until smooth. The plates were Dimethyl sulfoxide (DMSO) incubated for 4 hours in an incubator (CO_2 ٪ 5) at 37 ° C. Then, empty the whole medium, add (100) µl of DMSO to each well, and wait for the formazan crystals to dissolve to form a pink-purple solution. Then the light absorption of the samples was read at (570) nm using a Dana 3200 microplate reader, value was calculated with Prism software version 8.2.

3. Results and Discussion

The X-Ray diffraction analyses were done for the synthesized CuO NPs to confirm their crystalline nature. The results of the XRD analysis of the CuO NPs were interrelated with the Joint Committee on Powder Diffraction Standards (JCPDS), which confirmed the crystalline nature of CuO NPs (JCPDS 96- 901-5925) and (JCPDS 48-1548). Fig. 2 shows the XRD patterns at different frequencies of (4,6,8) Hz for the synthesized CuONPs.

The crystallite size was determined for different frequencies using the Scherrer formula, which is given by [8]:

$$D = \frac{0.9\,\lambda}{\beta\,\mathrm{Cos}\,\theta} \qquad (\mathbf{1})$$

where: λ is the wavelength of the X-ray, β is the FWHM, and θ is the Bragg angle. The structural property parameters are displayed in Table (2). For Cu films, the XRD results indicated that the crystallite size increase was frequency dependent.

The main characteristic diffraction peaks of the three samples were consistent, as shown in Fig. 2, and the corresponding 2θ is also consistent. The peaks of the copper oxide were 111, 002, and 020 corresponding to 2θ of 35.63°, 38.9°, and 52.65°, respectively.

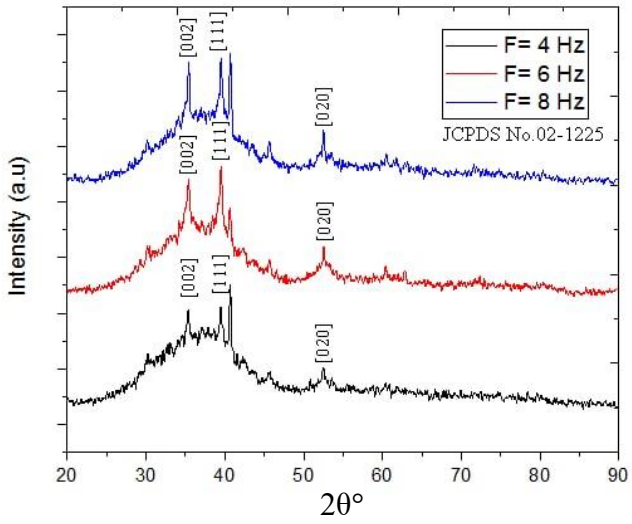

Figure 2: XRD patterns of CuO nanostructures at frequency of (4,6,8) Hz with laser energy of 400mJ.

***Table 2: The calculated values for the (CuO) peaks for frequency of 8Hz* in XRD.**

Sample	hkl	Frequency (Hz)	d(nm)	FWHM	2θ
CuO	110	8	22.92934	0.3739	33.54
CuO	111	8	25.11332	0.336	38.65
CuO	020	8	18.15219	0.4723	53.54

The morphology of nanocrystalline CuO thin film was examined using FESEM, as shown in Fig. 3. The sample formed at a f=4Hz was observed to have a surface with uniform grains but of small numbers. The increase in laser frequency (6, and 8 Hz) resulted in an increase in grain density, as it is evident from Table 2. The crystal size of copper nanoparticles ranged between (18-50) nm.

a b c

Figure 3: FESEM image for CuO nanoparticles at different frequencies (4,6,8) Hz with laser energy of 400mJ.

The Energy Dispersive X-ray (EDX) spectrum confirmed the presence of elemental gold (specific to the test device), copper and oxygen at different laser frequencies, as shown in Fig. 4. The energy is displayed on the horizontal axis in KeV, while the number of X-ray count rate is shown on the vertical axis. For CuO NPs, the weight and atomic percentage of copper (Cu) and oxygen (O) present in the samples were (82.0:18.0, 62.1:37.9, and 50.4:49.6) per cent for the different laser frequencies (4, 6 and 8) Hz, respectively; this demonstrates that the CuO thin films were free of contaminants.

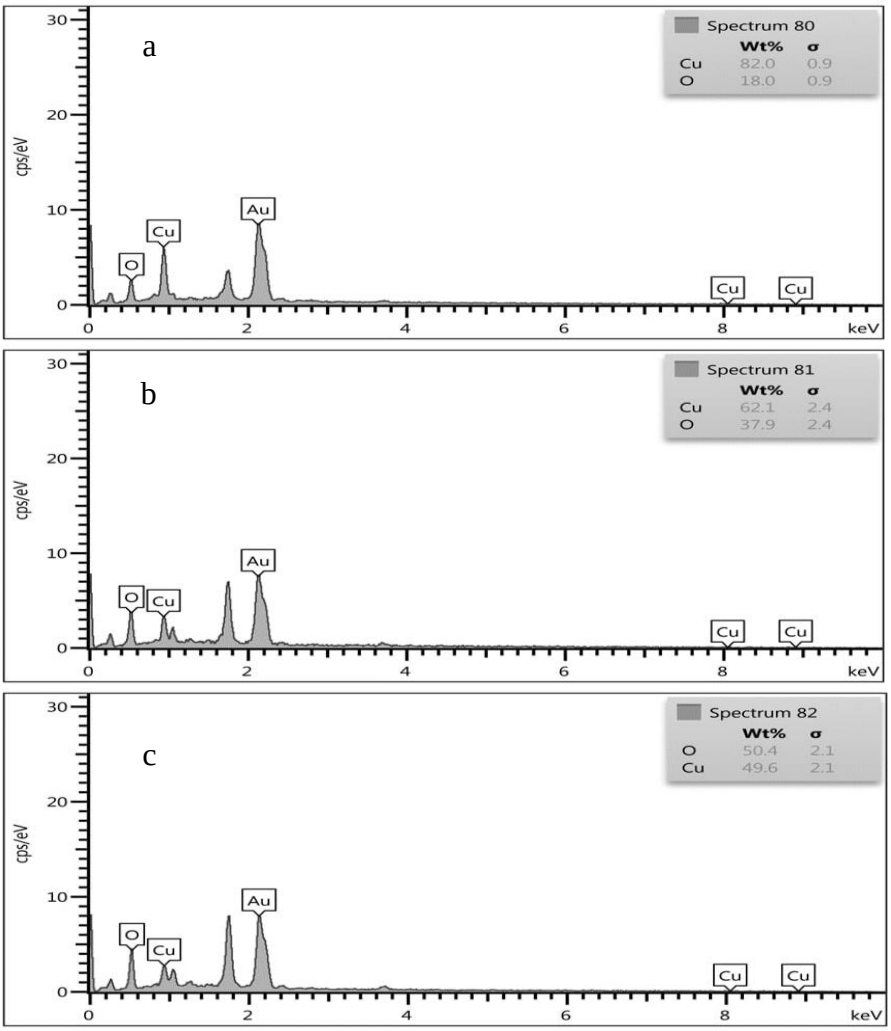

Figure 4: EDX pattern of CuO nanostructures at different frequencies (a) 4 (b) 6 (c) 8 Hz with laser energy of 400mJ.

3.1. Effects of CuONPs on liver Cancer (Hep-G2) Cell Line

Maximum cytotoxicity was 37.81 percent after 24 hours of incubation of (HepG-2) cells, whereas maximum viability was 62.19 percent, which was achieved at 500 µg mL^{-1} CuO concentration, as shown in Fig. 5.

3.2. Effects of CuONPs on normal (HdFn) cell line

Maximum cytotoxicity was 2.89 percent after 24 hours of incubation of (HdFn) cells, whereas maximum viability was 97.11 percent, which was achieved at 500 µg mL^{-1} CuO concentration, as illustrated in Fig. 6.

This in vitro study validated the selective effects of nanoparticles on cells. Nanotechnology has opened up a whole new area in cancer care by monitoring the release of the medication and lowering its side effects, i.e., cancer cells have been inhibited without harming normal cells, opened up a whole new sector in cancer care through regulating the delivery of medicine and lowering its side effects. Another aspect is that nanoparticles with a high surface-to-volume ratio aid distinct functional groups in attaching to such a nanoparticle and therefore tie tumor cells together. Because of the small nanoparticle size (under 100 nm) and the lack of a good tumor lymphatic drainage system, tumor cells can act as an active center for collecting nanoparticles [20]. Cytotoxicity is an essential factor in studying the activity of prepared nanomaterials on normal and cancer cells. Biologically, cytotoxicity is dependent on the production of

ROS. Aside from oxidative stress, other factors include dose, autophagy activation, exposure time, cell uptake, and substance concentration effects on the cytotoxicity [21, 22].

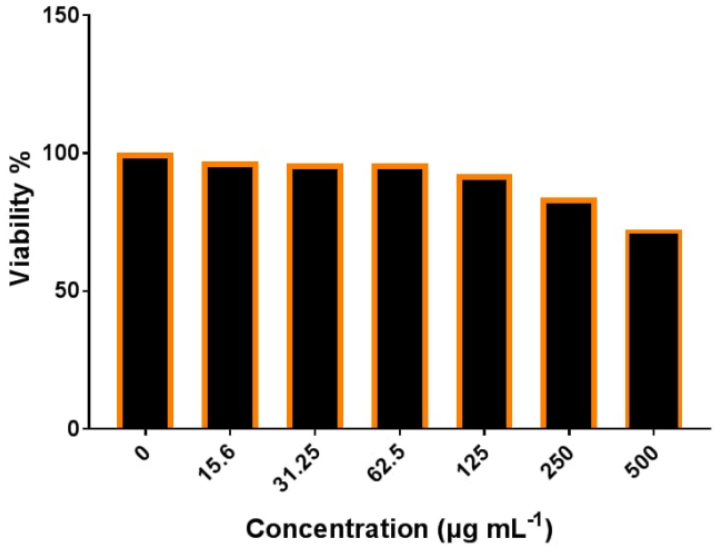

Figure 5: Cell viability rate of synthesis CuO nanoparticles for Hep-G2 Cell line.

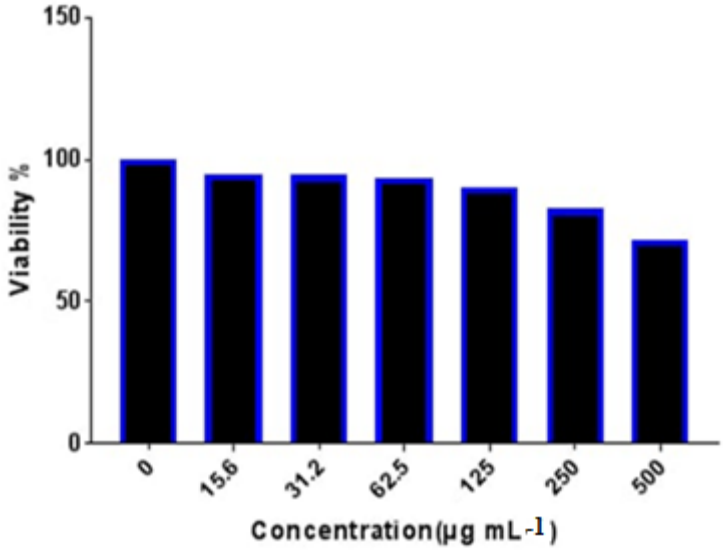

Figure 6: Viability of CuO NPs in (HdFn) cell line.

4. Conclusions

In terms of cost and speed, this approach has several advantages. The copper nanoparticles' crystal sizes ranged from (18 to 50) nm. The presence of copper and oxygen was confirmed in the prepared materials, which were free of impurities. The cytotoxic effects of CuO NPs on cancer cell lines (human Hep-G2 liver cancer) and normal cell lines (HdFn) were studied. The toxicity of CuONPs on the cancerous Hep-G2 cell line was 37.81 %, while that of the normal HdFn cell line was 27%. Although the toxicity on the cancer cells is higher, it is not effective to the extent required to kill cancer cells.

Acknowledgments

The authors gratefully acknowledge for each, University of Baghdad, College of Science for women, Department of Physics, Medical Physics Lab.

Conflict of interest

Authors declare that they have no conflict of interest

References

1. M. Bagherzadeh, M. Safarkhani, A. M. Ghadiri, M. Kiani, Y. Fatahi, F. Taghavimandi, H. Daneshgar, N. Abbariki, P. Makvandi, and R. S. Varma, Sci. Rep. **12**, 15351 (2022).
2. F. A. Bezza, S. M. Tichapondwa, and E. M. Chirwa, Sci. Rep. **10**, 16680 (2020).
3. Y. Ma, *Laser Technology and its Applications*. (London, UK, IntechOpen, 2019).
4. J. O. Ighalo, P. A. Sagboye, G. Umenweke, O. J. Ajala, F. O. Omoarukhe, C. A. Adeyanju, S. Ogunniyi, and A. G. Adeniyi, Envir. Nanotech., Monit. Manag. **15**, 100443 (2021).
5. C. Petridis, K. Savva, E. Kymakis, and E. Stratakis, J. Coll. Interf. Sci. **489**, 28 (2017).
6. S. N. Mazhir, N. A. Abdullah, A. F. Rauuf, A. H. Ali, and H. I. Al-Ahmed, Bagh. Sci. J. **15**, 81 (2018).
7. Z. Yan, R. Bao, and D. B. Chrisey, Phys. Chemis. Chem. Phys. **15**, 3052 (2013).
8. B. Bai, S. Saranya, V. Dheepaasri, S. Muniasamy, N. S. Alharbi, B. Selvaraj, V. S. Undal, and B. M. Gnanamangai, J. King Saud Univer.-Sci. **34**, 102120 (2022).
9. J. M. Gaucin-Delgado, A. Ortiz-Campos, L. G. Hernandez-Montiel, M. Fortis-Hernandez, J. J. Reyes-Pérez, J. A. Gonzáles-Fuentes, and P. Preciado-Rangel, Plants **11**, 912 (2022).
10. N. Acacia, F. Barreca, E. Barletta, D. Spadaro, G. Currò, and F. Neri, Appl. Surf. Sci. **256**, 6918 (2010).
11. D. Alagarasan, A. Harikrishnan, M. Surendiran, K. Indira, A. S. Khalifa, and B. H. Elesawy, Appl. Nanosci., 1 (2021).
12. N. K. Abdalameer and S. N. Mazhir, Inter. J. Nanosci. **20**, 2150044 (2021).
13. L. S. Alqarni, M. D. Alghamdi, A. A. Alshahrani, and A. M. Nassar, J. Chem. **2022**, 1 (2022).
14. Z. Alhalili, Arab. J. Chem. **15**, 103739 (2022).
15. R. Katwal, H. Kaur, G. Sharma, M. Naushad, and D. Pathania, J. Indus. Engin. Chem. **31**, 173 (2015).
16. S. Nations, M. Long, M. Wages, J. D. Maul, C. W. Theodorakis, and G. P. Cobb, Chemosphere **135**, 166 (2015).
17. S. N. Mazhir, K. A. Aadim, M. M. Al-Halbosiy, and N. K. Abdalameer, Indian J. Foren. Medic. Toxic. **15**, 2072 (2021).
18. Q. Zhang, K. Zhang, D. Xu, G. Yang, H. Huang, F. Nie, C. Liu, and S. Yang, Prog. Mat. Sci. **60**, 208 (2014).
19. V. A. Arzumanian, O. I. Kiseleva, and E. V. Poverennaya, Inter. J. Molec. Sci. **22**, 13135 (2021).
20. S. Khorrami, A. Zarrabi, M. Khaleghi, M. Danaei, and M. Mozafari, Inter. J. Nanomedic. **13**, 8013 (2018).
21. M. Ott, V. Gogvadze, S. Orrenius, and B. Zhivotovsky, Apoptosis **12**, 913 (2007).
22. A. Wongrakpanich, I. A. Mudunkotuwa, S. M. Geary, A. S. Morris, K. A. Mapuskar, D. R. Spitz, V. H. Grassian, and A. K. Salem, Envir. Sci.: Nano **3**, 365 (2016).

تحضير CuO النانوي بطريقة الاستئصال الليزر النبضي في السوائل و تاثيرها على الخلايا السرطانية في الكبد والقولون

هدى حسين عباس[1] ، صباح نوري مزهر[1]
[1]قسم الفيزياء، كلية العلوم للبنات، جامعة بغداد

الخلاصة

تم استخدام تقنية الاستئصال الليزر النبضي في السوائل في هذه الدراسة لتحضير جسيمات نانوية مستقرة وفعالة من حيث التكلفة من معدن النحاس النقي. تم فحص تركيب الجسيمات النانوية لأكسيد النحاس البلوري من خلال تقنيات تحليلية مختلفة مثل قياس تركيز الجسيمات باستخدام مطياف الامتصاص الذري، ومقياس حيود الأشعة السينية (XRD) لتحديد حجم البلورة وتحديدها. تم أيضًا فحص التركيب البلوري للجسيمات المحضرة، وفحص العينات بالماسح المجهر الإلكتروني FESEM، والسمية الخلوية للجسيمات النانوية. بعد 24 ساعة من التعرض تم حساب النسبة المئوية للسمية الخلوية، أذ كانت أقصى سمية لـ HepG-2 37.81٪ بتركيز 500 بعد 24 ساعة من التعرض. وايضا كانت السمية القصوى للخط الطبيعي 27.85٪ بتركيز 500.

الكلمات المفتاحيه: جسيمات اوكسيد النحاس النانويه، الاجتثاث بالليزر النبضي في السائل، سرطان الكبد، خطوط خلايا HdFn، تلألؤ ضوئي